

ORIGINAL RESEARCH ARTICLE

Experimental investigation of cutting force of powder metallurgy valve guide rod hole

Ahmed Qays Abdullah

Mechanical Engineering Department, College of Engineering AlShirqat, Tikrit University, Tikrit 34001, Iraq;
ahmed_qays@tu.edu.iq

ABSTRACT

Aiming at the problem of fast wear of machining tools in the special powder metallurgy valve guide rod hole and gasket seat of a certain engine cylinder head, in order to solve the technical problems in the cutting force (CF) of this kind of powder metallurgy materials, different tools are used and the analysis is carried out under different cutting test conditions. The cutting force law and surface roughness change law of similar powder metallurgy materials are determined to determine the appropriate tool materials and processing parameters. The experimental results show that under the same processing conditions, ceramic tools will suffer less than cemented carbide tools and cutting force can obtain a smaller surface roughness. In addition, the mass production process of valve seat, the blade material is ceramic knife.

Keywords: powder metallurgy; valve guide rod hole; washer seat; cutting characteristics

ARTICLE INFO

Received: 19 September 2023
Accepted: 7 October 2023
Available online: 30 April 2024

COPYRIGHT

Copyright © 2023 by author(s).
Applied Chemical Engineering is published
by EnPress Publisher, LLC. This work is
licensed under the Creative Commons
Attribution-NonCommercial 4.0 International
License (CC BY-NC 4.0).
<https://creativecommons.org/licenses/by-nc/4.0/>

1. Introduction

Powder metallurgy parts are widely used in automobiles and other industries, but powder forming equipment basically depends on imports, which greatly restricts the development of my country's powder metallurgy industry. Automobile engine valve seats, valve guides and other products have already used the powder metallurgy molding process in large quantities, which is a mature process technology^[1]. Powder metallurgy (PM)^[2] is to mix metal powder and metal powder or metal powder and non-metal powder according to the required ratio and then press into a mold cavity^[3], and then undergo high temperature sintering^[4-6] becomes a process of mechanical parts. It is a manufacturing process that saves materials, is efficient, has less pollution, and is suitable for mass production with little or no cutting. James^[7] studied the effect of copper infiltration on the properties of sintered steel, and pointed out that the material after copper infiltration showed excellent wear resistance. In particular, its residual porous structure makes it have good self-lubrication and sound insulation, making it widely used in many industries, especially the engine valve seat made of powder metallurgy has good overall performance and can meet its resistance requirements for wear, corrosion resistance and impact resistance. The material of the engine valve guide rod hole and valve seat ring of a certain equipment is powder metallurgy^[8]. Londhe^[9] found that the hardness and tensile strength of iron-based powder metallurgy materials after copper infiltration were significantly improved, and the wear resistance was increased by 2.5 to 3.3 times

compared with the base material. In addition, proportional valves, servo valves, and the application of electronic control system can greatly improve the performance of hydraulic powder metallurgy press^[10].

This paper is focused on fast tool wear in the machining of the cylinder head valve guide rod hole and gasket seat of a certain equipment. The detail studies of cutting special powder metallurgy materials problems^[11]. The law of CF and surface roughness analyzes during the cutting Laws, determine the appropriate tool material, and lay the foundation for the later design of a composite tool for deep hole machining.

2. Material and Experimental protocol

2.1. Experimental setup

Machine tool: C620-3 horizontal lathe; dynamometer: three-way piezoelectric crystal dynamometer 9257B. Cutting tools: Cermet blade FD22 and cemented carbide blade YT726. The main performance indicators of the selected tool materials are shown in **Table 1**, and the working angle is shown in **Table 2**. Cutting fluid: The experiment adopts dry cutting form. Cutting amount and requirements: The feed rate is respectively 0.05 mm/r, 0.1 mm/r, 0.16 mm/r, 0.2 mm/r, 0.25 mm/r; the cutting depth is 0.1 mm, 0.2 mm; the cutting speed (CS): each type of cutting Under the conditions, the CS of YT726 and FD22 are 62 m/min, 75 m/min, 106 m/min, 125 m/min, 150 m/min.

Table 1. Performance indicators of tool materials.

Tool material	Density (g/cm ³)	Hardness (HRA)	Bending strength (MPa)
FD22	4.75	94.5	850
YT726	13.6–14.5	92.0	1370

Table 2. Tool working angle index.

Tool material	Front angle γ_0	Back angle α_0	Blade inclination λ_s	Entering angle κ_r	Secondary declination κ_r'
FD22	-6°	6°	-6°	90°	10°
YT726	10°	11°	-3°	90°	8°

2.2. Principle of cutting force measurement system

The measuring method is to fix the tool on the dynamometer, and fix the dynamometer on the workbench of the lathe. As shown in **Figure 1**, the dynamometer used in the system is the three-way piezoelectric crystal dynamometer Kistler9257B, and the charge amplifier is Kistler5017B (The performance parameters are shown in **Table 3**).

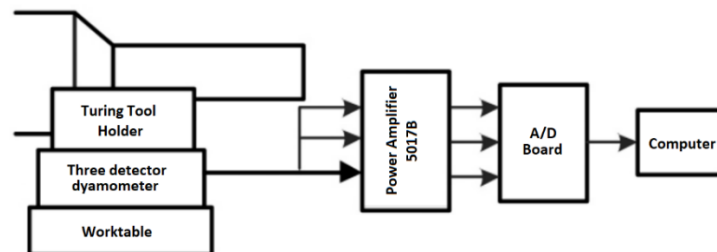


Figure 1. The turning force measurement system.

Table 3. Performance parameters of three-way piezoelectric crystal force gauge and charge amplifier.

Three-way piezoelectric crystal force		Power amplifier 5017B	
Range	F _x , F _y , F _z = -5–5 KN	Range	± 10–999000 pC
Sensitivity	F _x , F _y ≈ 7.5 pC/N; F _z ≈ 3.5 pC/N	Linearity error	≤ ± 5%

Natural frequency	$f_0 \approx 3.5\text{kHz}$	Bandwidth	0–200 kHz
Insulation resistance	> 1013	Drift	$< \pm 0.03\text{ pC/s}$
Stiffness	$C_x, C_y > 1\text{ kN}/\mu\text{m}; C_z > 2\text{ kN}/\mu\text{m}$	Time impedance	Long $> 1014\ \Omega$; Mid $\approx 1011\ \Omega$; short $\approx 1019\ \Omega$
Linearity	$\leq \pm 1\% \text{ FSO}$	Low pass filter	10 Hz–300 kHz

The measurement system has the advantages of large measuring range, good rigidity, high sensitivity, good dynamic response characteristics, wide frequency response range, good linearity, small drift, and good low-pass filtering performance. It can meet the requirements of milling force measurement. The CF signals in the three directions of X, Y, and Z are respectively input to the corresponding channels of the charge amplifier through high-impedance wires. The input signal is amplified by the charge amplifier, and the analog signal output from the charge amplifier is amplified by the A/D conversion board. Converted to digital signal. The force signal generated in the cutting process is first transformed into a charge signal through a force gauge, and then transformed into a voltage signal through a charge amplifier, and then sampled under computer control through a sampling board. The sampling frequency and time can be set by software. In order to accurately measure the dynamic changes of the milling force, a higher sampling frequency is adopted, namely $f_s = 20\text{ kHz}$, and the sampling time is 2 s.

3. Experimental results

3.1. Cutting force

The cutting conditions of **Figure 2** are: cutting speed $v_c = 62\text{ m/min}$, in the case of cutting depth $a_p = 0.1\text{ mm}$ and 0.2 mm , the influence of changing the feed amount on the main CF. The cutting conditions of **Figure 3** are: cutting depth $a_p = 0.2\text{ mm}$, in the case of feed $f = 0.1\text{ mm}$ and 0.2 mm , the effect of changing the CS on the main CF. When the cutting depth a_p and the feed amount f are constant, the main CF F_z decreases as the CS v_c increases. When the CS v_c and the cutting depth a_p are constant, the main cutting force F_z increases with the increase of the feed amount f .

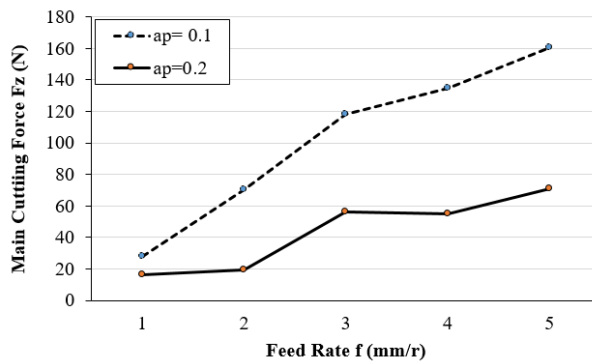


Figure 2. The influence of feed on the main cutting force.

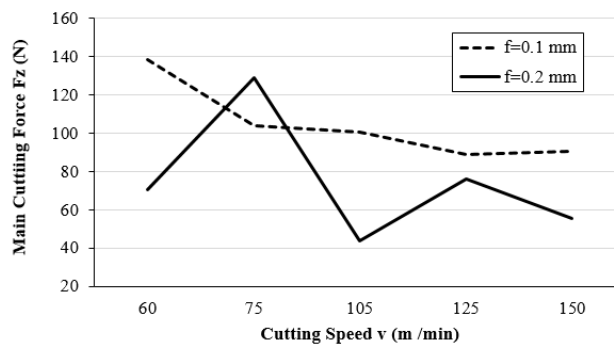


Figure 3. The influence of cutting speed on the main CF.

Figure 4 cutting conditions are: cutting depth $a_p = 0.2$ mm, in the case of feed $f = 0.1$ mm and 0.2 mm, the effect of changing the CS on the main CF. **Figures 2** and **4** show that the main CF F_z increases as the cutting depth a_p increases when the CS v_c and the feed amount f are constant. The cutting conditions of **Figure 5** are: cutting depth $a_p = 0.2$ mm, in the case of feed $f = 0.1$ mm, the influence of changing the CS on the main CF. Since the cutting edge of the ceramic tool has a negative chamfer, compared with the cemented carbide tool with a positive rake angle, the metal of the cut layer deforms more when cutting, so a relatively large CF should be generated. **Figure 5** shows that under the same cutting conditions, the main cutting force F_z of the selected two types of tool materials is similar. This is because Ti (C, N)-based cermets have higher cutting forces than cemented carbides. The red hardness, wear resistance, heat resistance and low coefficient of friction reduce the bonding between the chip and the tool, and the unit CF is small, so the main CF is reduced.

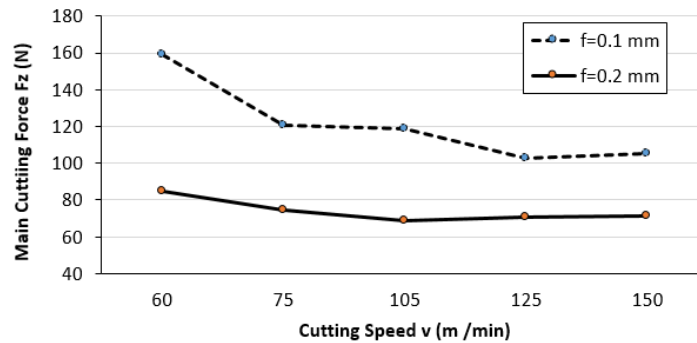


Figure 4. The influence of CS on the main cutting force.

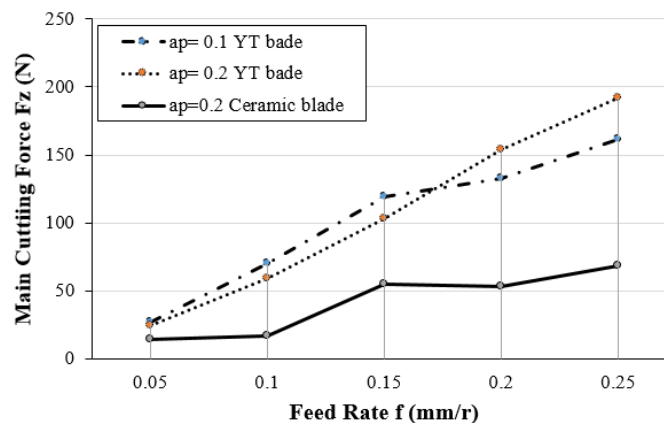


Figure 5. The influence of feed on the main cutting force.

3.2. Surface roughness

The cutting conditions of **Figure 6** are cutting depth $a_p = 0.2$ mm, in the case of feed $f = 0.1$ mm, the effect of changing the CS on the main CF. **Figure 7** are: The cutting conditions of cutting depth $a_p = 0.2$ mm, under the condition of CS $v_c = 106$ m/min, changing the influence of CS on the main CF.

Figures 6 and **7** show that under the same conditions, the surface roughness R_a value of the workpiece processed with the ceramic knife FD22 is smaller than the surface roughness R_a value of the workpiece processed with the cemented carbide knife YT726, so it is necessary to obtain a smaller value for roughness, ceramic blades should be used as much as possible. The roughness measurement results show that the feed rate has a greater impact on the surface roughness of the machined surface. The larger the feed rate, the higher the roughness value, while the CS has a small effect on the surface roughness. The surface roughness of the cermet tool is significantly lower than that of YT cemented carbide tools.

There are two main reasons: the first because the cermet cutter adopts negative rake angle cutting, it has a strong squeezing effect on the machined surface and changes the porous structure of the powder metallurgy

material itself. The structure reduces the roughness of the machined surface; the second reason it is because the friction coefficient between the cermet tool and the machined part is small; it is not easy for the chips to form a stagnant layer on the rake surface, which is also conducive to reducing the surface roughness.

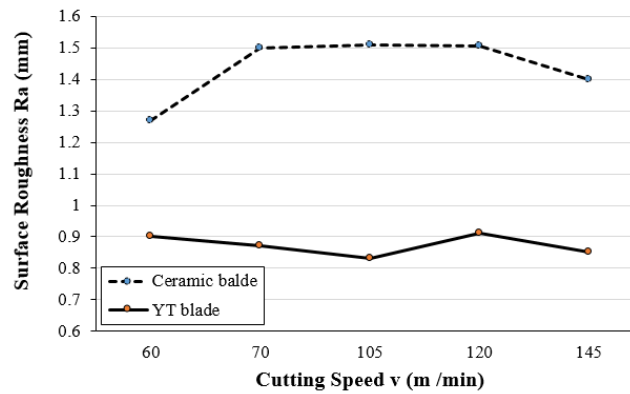


Figure 6. The effect of CS on surface roughness.

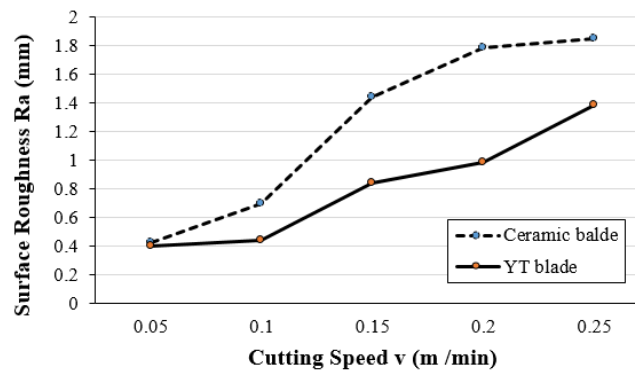


Figure 7. The influence of feed on surface roughness.

4. Conclusions

This paper investigates the CF and surface roughness, the main conclusions can be: When using cermet cutter blades and cemented carbide blades to cut powder metallurgical materials for engine valve seats of certain equipment, the main CF will increase with the feed rate. In addition, the depth of cut increases, but decreases with the increase of CS; the surface roughness value will increase with the increase of the feed, and the CS has little effect on the surface roughness; Under the same processing conditions, ceramic knives will receive a smaller CF than cemented carbide knives and obtain a smaller surface roughness.

Conflict of interest

The author declares no conflict of interest.

References

1. Martin P, Salvo C, Pio E, et al. A Study on the Phase Formation and Magnetic Properties of FeNiCoCuM (M = Mo, Nb) High-Entropy Alloys Processed Through Powder Metallurgy. *Metallurgical and Materials Transactions A*. 2021, 52(3): 1044-1058. doi: 10.1007/s11661-021-06137-4
2. Abolkassem SA, Mohamed LZ, Gaber GA, et al. Microstructure and corrosion behavior of FeNiCoCrCu and FeNiCoCrMn high entropy alloys manufactured by powder metallurgy in different acid media. *Journal of Materials Research and Technology*. 2021, 10: 1122-1142. doi: 10.1016/j.jmrt.2020.12.016
3. You D, Wang Y, Yang C, et al. Comparative analysis of the hot-isostatic-pressing densification behavior of atomized and milled Ti6Al4V powders. *Journal of Materials Research and Technology*. 2020, 9(3): 3091-3108. doi: 10.1016/j.jmrt.2020.01.055

4. Kruzhanov VS. Modern Manufacturing of Powder-Metallurgical Products with High Density and Performance by Press–Sinter Technology. *Powder Metallurgy and Metal Ceramics*. 2018, 57(7-8): 431-446. doi: 10.1007/s11106-018-0002-1
5. Qin H, Xu R, Lan P, et al. Wear Performance of Metal Materials Fabricated by Powder Bed Fusion: A Literature Review. *Metals*. 2020, 10(3): 304. doi: 10.3390/met10030304Herbert
6. Danningera H, Weissb B. *High Cycle Fatigue of Powder Metallurgy Materials*. VIII Congreso Nacional de Propiedades Mecánicas de Sólidos, Gandia; 2002. pp. 195-204
7. James WB. Hoeganaes Corporation. *Powder Metallurgy Methods and Applications*. ASM Handbook; 2015.
8. Mohammed MN, Yusoh KB, Ismael MN, Shariffuddin JHBH. Synthesis of thermo-responsive poly(N-vinylcaprolactam): RSM-based parameters optimization. *Multiscale and Multidisciplinary Modeling, Experiments and Design*. 2019, 2(3): 199-207. doi: 10.1007/s41939-019-00045-2
9. Londhe RT. Experimental Analysis of Valve and Valve Seats Wear in Gases (CNG) Fuelled Engine. *IOSR Journal of Mechanical and Civil Engineering*. 2014, 11(4): 56-62. doi: 10.9790/1684-11415662
10. Gomes MP, dos Santos IP, Couto CP, et al. Heat Treatment of Sintered Valve Seat Inserts. *Materials Research*. 2018, 21(5). doi: 10.1590/1980-5373-mr-2018-0068
11. Madej M, Leszczyńska-Madej B, Garbiec D. High Speed Steel with Iron Addition Materials Sintered by Spark Plasma Sintering. *Metals*. 2020, 10(11): 1549. doi: 10.3390/met10111549